Journal of Materials Chemistry C

PAPER

View Article Online
View Journal

Cite this: DOI: 10.1039/c5tc01657f

4-Diphenylamino-phenyl substituted pyrazine: nonlinear optical switching by protonation†

Liang Xu,‡[a] Hai Zhu,‡[b] Guankui Long,[a] Jun Zhao,[c] Dongsheng Li,[c] Rakesh Ganguly,[d] Yongxin Li,[d] Qing-Hua Xu*[b] and Qichun Zhang*[ad]

Received 5th June 2015,
Accepted 10th August 2015

DOI: 10.1039/c5tc01657f

www.rsc.org/MaterialsC

Through the integration of a 4-diphenylamino-phenyl unit with a pyrazine segment, a series of novel organic conjugated molecules with different spacers and shapes have been synthesized and fully characterized. These as-prepared compounds exhibit reversible acidochromism in response to protonation and deprotonation. The investigation of the nonlinear optical (NLO) properties reveals that the neutral forms of these structures display a reverse saturated absorption (RSA), while the protonated forms show a saturated absorption (SA).

Introduction

Two-photon absorption (TPA) is a third-order nonlinear optical (NLO) process, where two photons are absorbed simultaneously to promote a molecule from the ground state to the excited state.[1] Normally, organic molecules with large TPA cross sections are important for their potential applications in two-photon fluorescence imaging,[2] optical power limiting,[3] two-photon photodynamic therapy (PDT),[4] optical data storage,[5] and photo switching.[6] TPA cross-section strongly depends on the extent of intramolecular charge transfer characteristics of molecules.[7] For example, the TPA cross section of fluorescein (water, pH ~ 13 800 nm),[8] Rhodamine B (methanol, 800 nm),[9] and Rhodamine 6G (methanol, 802 nm)[10] is reported to be 36, 150 and 134 GM, respectively. From the viewpoint of the design of TPA molecules, their structural factors should include the effective conjugation and the polarizability.[11] Currently, D–A molecules, which consist of electron donors and electron acceptors connected by a π-conjugated spacer, are the most important class of TPA chromophores.[12] The relationship between the structure and NLO properties has been strongly investigated by various classes of conjugated organic molecules with different conjugation lengths, as well as the strength and substitution patterns of donors and acceptors.[13] Usually, through increasing the length of the π-spacer in D–π–A systems, the ground-state D–A conjugation is reduced and the HOMO–LUMO gap decreases.[14] Therefore, efforts to further increase the nonlinearity are usually focused on increasing the conjugation length or increasing the strength of donors or acceptors or both.[15]

Besides the conjugation length, the structures of the π-conjugated bridges should also be considered in designing nonlinear optical materials because this factor would also affect the intramolecular charge transfer.[16] Recently, some studies on the novel structures and conjugation patterns of the NLO chromophores have been reported.[17] The strategy to form a rigid structure through fusing the donor and the acceptor together into one system has been proven to be a smart way to tune the electro-optical properties. On one hand, the direct attachment of the donor onto the acceptor unit facilitates a strong donor–acceptor interaction; on the other hand, such an arrangement is helpful to achieve a lower band gap and balance dual charge transport properties.[18] Because the 4-diphenylamino-phenyl group is a strong electron donor and pyrazine is an electron acceptor,[19] the 4-diphenylamino-phenyl substituted pyrazine is predicted to have great performance in NLO applications.[20] Moreover, such a rigid planar structure has a great contribution to the extended π-electron delocalization, where p-orbitals in nitrogen centers can effectively mix with π-electrons. Furthermore, the electro-optical properties could be modulated using an external trigger.[21] In addition, the behavior of the acceptor pyrazine could be altered by protonation and such alteration could lead to NLO response at the molecular level. Note that such NLO variations in response to protonation–deprotonation would make this material a potential candidate for the application

[a] School of Materials Science and Engineering, Nanyang Technological University, Singapore 639798, Singapore. E-mail: qczhang@ntu.edu.sg
[b] Department of Chemistry, National University of Singapore, 3 Science Drive 3, Singapore 117543, Singapore. E-mail: chmxqh@nus.edu.sg
[c] College of Materials and Chemical Engineering, Hubei Provincial Collaborative Innovation Center for New Energy Microgrid, China Three Gorges University, Yichang 443002, P. R. China
[d] Division of Chemistry and Biological Chemistry, School of Physical and Mathematic Sciences, Nanyang Technological University, Singapore 637371, Singapore

† Electronic supplementary information (ESI) available: Synthesis, characterization, photophysical properties, and the theoretical study of compounds **1–3**. CCDC 1403860–1403862. For ESI and crystallographic data in CIF or other electronic format see DOI: 10.1039/c5tc01657f

‡ The two authors have equal contribution to this paper.

in photo switching. Nonlinear optical switching effects are reported in various materials, such as graphene oxide films,[22] gold nanoparticles,[23] Rhodamine B[24] *etc.* These materials display a competition between saturable absorption (SA) and reverse saturable absorption (RSA) as the excitation fluence increased. Besides this excitation fluence based switching, a variety of methods[25] are employed to switch quadratic and cubic nonlinear optical properties, such as oxidation/reduction, photoisomerization sequences, and protonation/deprotonation. Protonation induced switching effects are previously demonstrated to display a reversible luminescent and second-order nonlinear property.[25a] To the best of our knowledge, there is no report on the nonlinear optical switching between SA and RSA by reversible protonation and with similar molecular structures. In this research, several 4-diphenylamino-phenyl substituted pyrazines with different moieties and shapes have been prepared and their NLO properties with switching behaviors are also investigated.

Results and discussion

As shown in Scheme 1, the starting material 4,4′-bis(*N*,*N*-diphenylamino)benzyl was prepared from triphenylamine and oxalyl chloride through Friedel–Crafts acylation.[26] Compounds **1–3** are synthesized by condensing 4,4′-bis(*N*,*N*-diphenylamino)benzyl and different kinds of diamines including 1,2-diaminobenzene, 4,5-dimethyl-1,2-phenylenediamine or 1,2-diaminoanthraquinone in acetic acid with a catalytic amount of IBX.[27]

Suitable crystals of compounds **1–3** (CCDC number: 1403860–1403862) for single crystal X-ray diffractometer analysis have been obtained by slow evaporation of dichloromethane solutions over two weeks. As shown in Fig. 1, for compounds **1–3**, the length of the C–C bond connecting the pyrazine ring to the 4-diphenylamino-phenyl group (1.48–1.49 Å) is between the average bond length of the C–C single bond and the aromatic C–C bond (C–C single bond 1.54 Å; double bond 1.33 Å; aromatic 1.40 Å).[28] The length of the C–N bond within the 4-diphenylamino-phenyl group (1.41–1.43 Å) falls close to the average aromatic C–N bond length (C–N single bond 1.47 Å; double bond 1.34 Å; aromatic 1.43 Å). Especially for compound **3**, the shortest C–N bond within the 4-diphenylamino-phenyl group is 1.38 Å, exhibiting a characteristic C–N double bond.

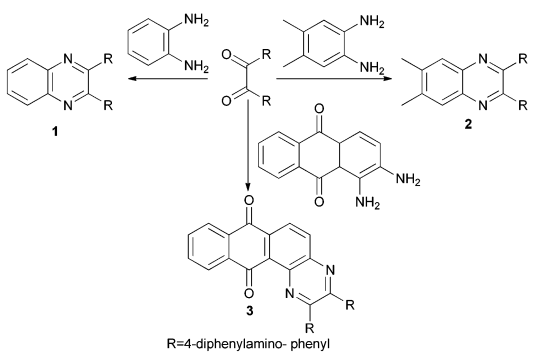

Scheme 1 Synthetic route for compounds **1–3**. Conditions: anhydrous acetic acid, Ar_2, 2-iodoxybenzoic acid, 120 °C, 24 h.

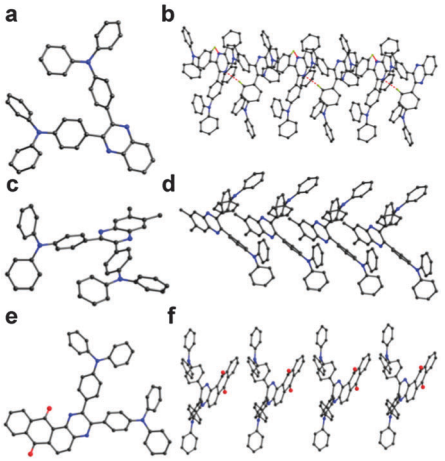

Fig. 1 The crystal structures of compounds **1–3** (a, c and e) and the crystal packing diagrams of compounds **1–3** (b, d and f).

Those phenomena indicate that the lone pair electrons on the nitrogen center of the 4-diphenylamino-phenyl group are delocalized into the pyrazine segment due to the electron-accepting tendency of the pyrazine.

Furthermore, the pyrazine ring and the phenyl ring directly connecting to it are twisted from each other with interplanar angles of 27.03° and 73.43°, which suggests a decoupling effect between the electron donor 4-diphenylamino-phenyl group and the electron acceptor pyrazine. The packing diagrams for compounds **1–3** are also shown in Fig. 1. Note that compound **1** forms a N–H–C weak hydrogen bond.

As shown in Fig. 2, compound **3** exhibits a broad and moderately intense absorption band (>500 nm), while compounds **1** and **2** show a relatively narrow absorption band (~400 nm). The peak positions of this band suggest a trend (**2** < **1** < **3**), reflecting the substituent effect on the electronic properties. Considering the phenylene moiety in compound **1** is a neutral group and the dimethylphenylene moiety in compound **2** is a weak electron donor, we believe that the electron push–pull system between the 4-diphenylamino-phenyl group

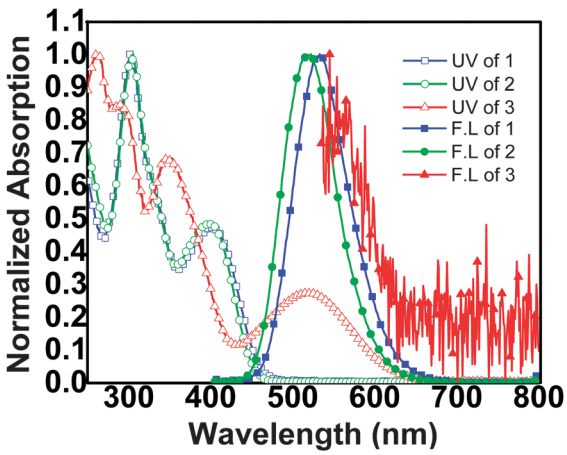

Fig. 2 The normalized UV-Vis and fluorescence spectra of compounds **1–3**.

and pyrazine is not significantly altered by the substituents. However, for compound **3**, the 9,10-dioxo-9,10-dihydro-anthracenyl moiety is a strong electron acceptor, which can effectively enhance the interaction between the electron donor and the acceptor, resulting in a bathochromic absorption shift. Note that, the absorption bands show a remarkable red shift when trifluoroacetic acid (TFA) was added to the solution containing compound **1**, **2** or **3** (Fig. S2, ESI†). The reason is that the N–H hydrogen bond is formed between the nitrogen of pyrazine and the hydrogen of TFA, generating a strongly electron-withdrawing pyrazinium ion, which triggered a strong intramolecular charge transfer between the amine donor and the pyrazinium acceptor. Through an aromatic conjugation, the amine loses one electron and turns into a strong electron acceptor, while the pyrazinium ion gets one electron and turns into electron donor amine. This aromatic conjugation stabilizes the LUMO and causes a dramatic red-shift of the absorption band. Meanwhile, it induces the dipole moments with reversed directions. For the 4-diphenylamino-phenyl segment, the nitrogen cannot be protonated due to the steric effect. The pyrazine is protonated to pyrazinium for compounds **1** and **2** while the anthraquinone is protonated to semiquinone for compound **3**. The protonation is completed upon the addition of 1000 equivalents of TFA. The isosbestic points indicate the presence of the neutral and protonated forms in equilibrium and the latter being predominant at higher concentrations of TFA (Fig. 3). In dichloromethane solutions, upon the addition of TFA, compounds **1** and **2** display a color change from yellow to violet, while the color of compound **3** changes from red to green. The original color could be regained by the addition of trimethylamine (TEA).

UV-Vis spectra of the titration of compound **1** through adding TFA and TEA are shown in Fig. 3. Upon the addition of TFA to the solution of compound **1**, there is a continuous decrease of the absorption peaks at 302 and 399 nm, followed by a continuous increase of the absorption peaks at 338 and 550 nm. Meanwhile, when TFA was added to the solution of compound **1**, the emission intensity decreased sharply (Fig. S2, ESI†). The specific data are shown in Table 1. It seems that the protonated species has a more pronounced dipolar relaxation from the excited state due to the presence of strong donor–acceptor interactions.

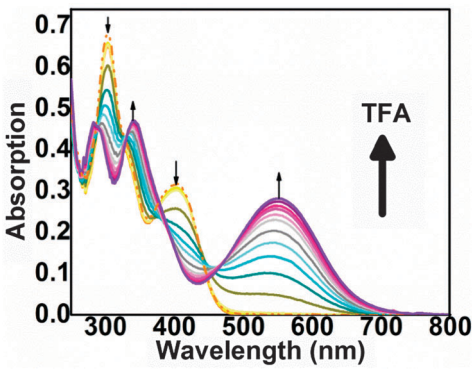

Fig. 3 The UV-Vis spectra of compound **1** upon adding TFA (the solid line) and TEA (the dotted line).

Table 1 The UV-Vis and fluorescence data of compounds **1–3** before and after adding TFA

	Abs. λ_{max} (nm)	Abs. λ_{max} (nm) (+1000 eq. TFA)	Fluor. λ_{max} (nm)	(Phi)n	(Phi)n (+1000 eq. TFA)
1	399	550	533	0.41	0.20
2	398	540	522	0.97	0.19
3	523	702	—	<0.01	<0.01

The oxidation and reduction potentials were measured using a cyclic voltammetric method. As shown in Fig. 4, all compounds show irreversible oxidation waves due to the removal of an electron from the 4-diphenylamino-phenyl group. The oxidation and reduction potentials are affected by the nature of the electronic interaction between the donor 4-diphenylamino-phenyl group and the acceptor. For compounds **1** and **2**, no reduction wave is monitored while two reversible reduction waves are found in compound **3** (Table 2).

The optimization for geometric structures of compounds **1–3** was carried out using the Gaussian 09 program at the B3LYP/6-31G* level (Table 3). And the frequency analysis was employed at the same level of theory to check whether the

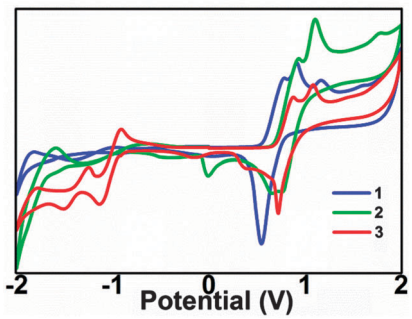

Fig. 4 The CV spectra of compounds **1–3**. The working electrode is glassy carbon; the counter electrode and the reference electrode are platinum wires. Potentials are recorded *versus* Fc^+/Fc in a solution of anhydrous dichloromethane (DCM) with 0.1 M tetrabutylammonium hexafluorophosphate ($TBAPF_6$) as a supporting electrolyte at a scan rate of 50 mV s^{-1}.

Table 2 The CV data of compounds **1–3**

	E^1_{ox}/V	E^2_{ox}/V	E^3_{ox}/V	E^1_{red}/V	E^2_{red}/V
1	0.42	0.70	0.94	—	—
2	0.53	0.86	1.36	—	—
3	0.54	0.84	—	−1.09	−1.54

Table 3 The calculated data of neutral and protonated forms of compounds **1–3**

	HOMO (eV)	LUMO (eV)	Gap (eV)
1	−4.90	−1.79	3.11
1(H$^+$)	−7.22	−5.60	1.62
2	−4.84	−1.65	3.19
2(H$^+$)	−7.10	−5.44	1.66
3	−4.98	−2.85	2.12
3(H$^+$)	−7.06	−6.14	0.92

optimized geometrical structure is at a stable point and evaluate the zero-point vibration energy (ZPE). The excess charges upon protonation were analyzed through mulliken population analysis (Fig. S3-1 and Table S3-1, ESI†). Upon protonation, the positive charge mainly delocalized on the quinoxaline (compounds **1** and **2**) and anthracene-9,10-dione (compound **3**) units. This is also consistent with the calculated results, the excess positive charges ($q > 0.3\ e$) mainly locate at the certain position of compounds **1**($\mathbf{H^+}$), **2**($\mathbf{H^+}$) and **3**($\mathbf{H^+}$), respectively. The calculated reaction free energy (ΔG) was summarized in Table S3-2 (ESI†). The electronic distributions in HOMO and LUMO for these compounds are shown in Fig. 5. The HOMOs of these compounds are delocalized over the 4-diphenylamino-phenyl groups, and are extended to the bridge, while the LUMOs are delocalized on the pyrazine and anthraquinone. The distribution of the HOMO and the LUMO is not totally separated within the molecule and a part of overlap is present, which suggests that the HOMO–LUMO transitions cannot be considered as pure charge transfer transitions and can be treated as π–π* transitions with prominent charge transfer contribution. Because the relationship between structure–electronic properties could be revealed by DFT calculation, the protonated forms of these compounds are also investigated. Except for slight structural variations, no obvious alternations in the geometry were observed after protonation. However, obvious changes in the electron distributions were observed for these compounds due to protonation. After protonation, the HOMO is concentrated on one 4-diphenylamino-phenyl segment, while the LUMO is extended to the benzene ring of the other 4-diphenylamino-phenyl group. All these changes indicate that the protonation of pyrazine enhances the electron-withdrawing ability and drifts the electron-density toward the pyrazinium ion.

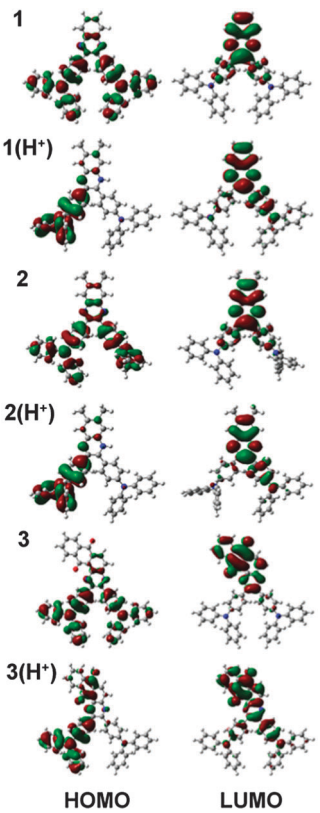

Fig. 5 The HOMO and the LUMO of neutral and protonated forms of compounds **1–3**.

The NLO properties of compounds **1–3** were characterized by an open aperture *z*-scan measurement, shown in Fig. S4-1 (ESI†). The open aperture *z*-scan measurements of compounds **1–3** are shown in Fig. 6. All the compounds exhibit reverse saturate absorption (RSA) under an excitation power density of 80 GW cm^{-2}. Interestingly, they switch from RSA to saturate absorption (SA) after protonation by adding 1000 eq. TFA into the solutions. The influence from both the solvents (CH_2Cl_2 and TFA) was ruled out based on *z*-scan curves of the solvents.

Under the assumption of a spatially and temporally Gaussian laser beam, the normalized beam transmittance is expressed by:[22,29]

$$T(z) = \frac{1}{\sqrt{\pi} q_0(z)} \int_{-\infty}^{\infty} \ln\left[1 + q_0(z) e^{-\tau^2}\right] d\tau$$

$$q_0(z) = \beta I(z) L_{\text{eff}}$$

$$I(z) = I_0 / \left(1 + z^2 / {z_0}^2\right)$$

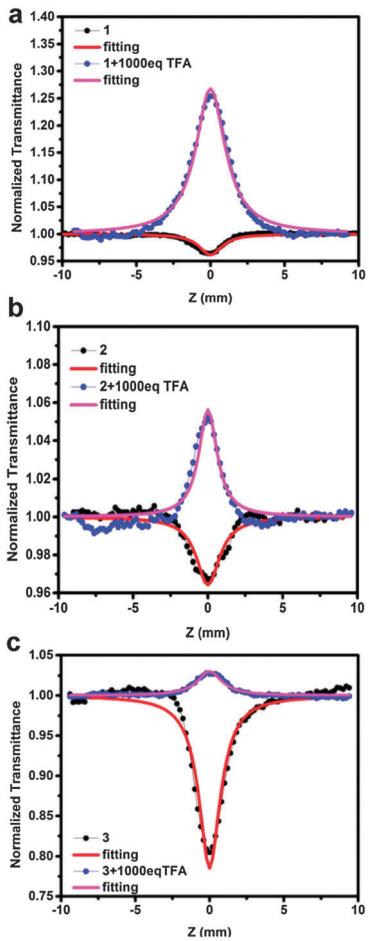

Fig. 6 The open aperture *z*-scan measurement of compounds **1–3** (a–c).

Table 4 The calculated nonlinear coefficient β and corresponding 2PA cross section $\sigma^{(2)}$ for compounds **1–3** and their protonated forms

	β (cm^{-1} GW^{-1})	$\sigma^{(2)}$ (GM)
1	0.833	34.3
1(H$^+$)	−15.5	—
2	0.784	32.3
2(H$^+$)	−0.913	—
3	5.14	211
3(H$^+$)	−0.674	—

where z is the distance between the sample and the focus; z_0 is the Rayleigh diffraction length; I_0 is the peak power density; L_{eff} is the effective interaction length and β is the nonlinear absorption coefficient. A positive β describes the two photon absorption (2PA) of the molecules, while, β is negative in the case of SA. The saturation intensity term is omitted in this study due to a rather low linear absorption coefficient at 800 nm.

Using this model, the calculated 2PA cross sections of compounds **1–3** are 34, 32 and 211. And the calculated nonlinear coefficient β and corresponding 2PA cross section $\sigma^{(2)}$ are listed in Table 4. In the case of 2PA, as the nonlinear absorption coefficient is inversely proportional to the energy difference between the LUMO and the virtual state induced by excitation, compound **3** possesses a larger 2PA cross section than **1** and **2** (ESI† S4).

After protonation, compounds **1–3** show switching from RSA to SA. This switching is due to the decrease of the gap between the HOMO and the LUMO of the compounds as discussed above. As the gap decreases after protonation, one photon absorption transition becomes possible. Electrons on the HOMO are excited to the LUMO transiently thus the HOMO is depleted and it shows a SA z-scan curve. The TFA concentration dependence z-scan curves are shown in Fig. S4-2 (ESI†). The RSA gradually switches to SA as protonation by TFA.

Conclusions

A series of novel 4-diphenylamino-phenyl substituted pyrazines have been obtained by one-step reaction between 1,2-diamine and 1,2-diketones. All compounds have been demonstrated to show unique properties for NLO applications. Upon the addition of trifluoroacetic acid and triethylamine, these compounds were subject to protonation and deprotonation on the pyrazine unit. In the neutral forms, compounds **1–3** exhibited reverse saturated absorption (RSA) with a 2TPA cross section of 34, 32 and 211 GM, respectively, while in the protonated forms, they display saturable absorption (SA). These results suggest that 4-diphenylamino-phenyl substituted pyrazines could have potential applications in reversible and highly efficient nonlinear optical switches.

Acknowledgements

Q.Z. acknowledges the financial support AcRF Tier 1 (RG 133/14) and Tier 2 (ARC 20/12 and ARC 2/13) from MOE, CREATE program (Nanomaterials for Energy and Water Management) from NRF, and New Initiative Fund from NTU, Singapore.

Notes and references

1 H. S. Nalwa, *Adv. Mater.*, 1993, **5**, 341–358.
2 (*a*) W. Denk, J. Strickler and W. Webb, *Science*, 1990, **248**, 73–76; (*b*) M. Velusamy, J.-Y. Shen, J. T. Lin, Y.-C. Lin, C.-C. Hsieh, C.-H. Lai, C.-W. Lai, M.-L. Ho, Y.-C. Chen, P.-T. Chou and J.-K. Hsiao, *Adv. Funct. Mater.*, 2009, **19**, 2388–2397; (*c*) L. Xu, Y. Zhao, G. Long, Y. Wang, J. Zhao, D. Li, J. Li, R. Ganguly, Y. Li, H. Sun, X.-W. Sun and Q. Zhang, *RSC Adv.*, 2015, **5**, 63080.
3 (*a*) H. Zhang, D. E. Zelmon, L. Deng, H.-K. Liu and B. K. Teo, *J. Am. Chem. Soc.*, 2001, **123**, 11300–11301; (*b*) C. W. Spangler, *J. Mater. Chem.*, 1999, **9**, 2013–2020.
4 J. Arnbjerg, A. Jiménez-Banzo, M. J. Paterson, S. Nonell, J. I. Borrell, O. Christiansen and P. R. Ogilby, *J. Am. Chem. Soc.*, 2007, **129**, 5188–5199.
5 (*a*) B. H. Cumpston, S. P. Ananthavel, S. Barlow, D. L. Dyer, J. E. Ehrlich, L. L. Erskine, A. A. Heikal, S. M. Kuebler, I. Y. S. Lee, D. McCord-Maughon, J. Qin, H. Rockel, M. Rumi, X.-L. Wu, S. R. Marder and J. W. Perry, *Nature*, 1999, **398**, 51–54; (*b*) S. Kawata and Y. Kawata, *Chem. Rev.*, 2000, **100**, 1777–1788.
6 (*a*) M. Irie, T. Fukaminato, T. Sasaki, N. Tamai and T. Kawai, *Nature*, 2002, **420**, 759–760; (*b*) M. Böckmann, N. L. Doltsinis and D. Marx, *Angew. Chem., Int. Ed.*, 2010, **49**, 3382–3384; (*c*) B. Champagne, A. Plaquet, J.-L. Pozzo, V. Rodriguez and F. Castet, *J. Am. Chem. Soc.*, 2012, **134**, 8101–8103; (*d*) F. Castet, V. Rodriguez, J.-L. Pozzo, L. Ducasse, A. Plaquet and B. Champagne, *Acc. Chem. Res.*, 2013, **46**, 2656–2665; (*e*) Y. Wu, Z. Yin, J. Xiao, Y. Liu, F. Wei, K. J. Tan, C. Kloc, L. Huang, Q. Yan, F. Hu, H. Zhang and Q. Zhang, *ACS Appl. Mater. Interfaces*, 2012, **4**, 1883–1886; (*f*) P. Serra-Crespo, M. A. van der Veen, E. Gobechiya, K. Houthoofd, Y. Filinchuk, C. E. A. Kirschhock, J. A. Martens, B. F. Sels, D. E. De Vos, F. Kapteijn and J. Gascon, *J. Am. Chem. Soc.*, 2012, **134**, 8314–8317.
7 M. A. Albota, C. Xu and W. W. Webb, *Appl. Opt.*, 1998, **37**, 7352–7356.
8 C. Xu and W. W. Webb, *J. Opt. Soc. Am. B*, 1996, **13**, 481–491.
9 D. Oulianov, I. Tomov, A. Dvornikov and P. Rentzepis, *Opt. Commun.*, 2001, **191**, 235–243.
10 J. Yoo, S. K. Yang, M.-Y. Jeong, H. C. Ahn, S.-J. Jeon and B. R. Cho, *Org. Lett.*, 2003, **5**, 645–648.
11 J. W. Baur, M. D. Alexander, M. Banach, L. R. Denny, B. A. Reinhardt, R. A. Vaia, P. A. Fleitz and S. M. Kirkpatrick, *Chem. Mater.*, 1999, **11**, 2899–2906.
12 A. Abbotto, L. Beverina, R. Bozio, A. Facchetti, C. Ferrante, G. A. Pagani, D. Pedron and R. Signorini, *Chem. Commun.*, 2003, 2144–2145.
13 (*a*) M. Albota, D. Beljonne, J.-L. Brédas, J. E. Ehrlich, J.-Y. Fu, A. A. Heikal, S. E. Hess, T. Kogej, M. D. Levin, S. R. Marder, D. McCord-Maughon, J. W. Perry, H. Röckel, M. Rumi,

G. Subramaniam, W. W. Webb, X.-L. Wu and C. Xu, *Science*, 1998, **281**, 1653–1656; (*b*) A. Adronov, J. M. J. Fréchet, G. S. He, K.-S. Kim, S.-J. Chung, J. Swiatkiewicz and P. N. Prasad, *Chem. Mater.*, 2000, **12**, 2838–2841; (*c*) M. M. Oliva, R. Juárez, M. Ramos, J. L. Segura, S. v. Cleuvenbergen, K. Clays, T. Goodson, J. T. L. Navarrete and J. Casado, *J. Phys. Chem. C*, 2013, **117**, 626–632.

14 B. A. Reinhardt, L. L. Brott, S. J. Clarson, A. G. Dillard, J. C. Bhatt, R. Kannan, L. Yuan, G. S. He and P. N. Prasad, *Chem. Mater.*, 1998, **10**, 1863–1874.

15 (*a*) T. Kogej, D. Beljonne, F. Meyers, J. W. Perry, S. R. Marder and J. L. Brédas, *Chem. Phys. Lett.*, 1998, **298**, 1–6; (*b*) M. Pawlicki, H. A. Collins, R. G. Denning and H. L. Anderson, *Angew. Chem., Int. Ed.*, 2009, **48**, 3244–3266.

16 H. Reyes, B. M. Munoz, N. Farfan, R. Santillan, S. Rojas-Lima, P. G. Lacroix and K. Nakatani, *J. Mater. Chem.*, 2002, **12**, 2898–2903.

17 (*a*) X.-H. Zhou, J. Davies, S. Huang, J. Luo, Z. Shi, B. Polishak, Y.-J. Cheng, T.-D. Kim, L. Johnson and A. Jen, *J. Mater. Chem.*, 2011, **21**, 4437–4444; (*b*) M. Shimada, Y. Yamanoi, T. Matsushita, T. Kondo, E. Nishibori, A. Hatakeyama, K. Sugimoto and H. Nishihara, *J. Am. Chem. Soc.*, 2015, **137**, 1024–1027; (*c*) S. Thomas, Y. A. Pati and S. Ramasesha, *J. Phys. Chem. A*, 2013, **117**, 7804–7809.

18 M. Barzoukas and M. Blanchard-Desce, *J. Chem. Phys.*, 2000, **113**, 3951–3959.

19 (*a*) K. Cao, J. Lu, J. Cui, Y. Shen, W. Chen, G. Alemu, Z. Wang, H. Yuan, J. Xu, M. Wang and Y. Cheng, *J. Mater. Chem. A*, 2014, **2**, 4945–4953; (*b*) H. Zhuang, Q. Zhang, Y. Zhu, X. Xu, H. Liu, N. Li, Q. Xu, H. Li, J. Lu and L. Wang, *J. Mater. Chem. C*, 2013, **1**, 3816–3824; (*c*) T. W. Holcombe, J.-H. Yum, J. Yoon, P. Gao, M. Marszalek, D. D. Censo, K. Rakstys, M. K. Nazeeruddin and M. Graetzel, *Chem. Commun.*, 2012, **48**, 10724–10726; (*d*) H.-W. Lin, L.-Y. Lin, Y.-H. Chen, C.-W. Chen, Y.-T. Lin, S.-W. Chiu and K.-T. Wong, *Chem. Commun.*, 2011, **47**, 7872–7874; (*e*) E. Ripaud, T. Rousseau, P. Leriche and J. Roncali, *Adv. Energy Mater.*, 2011, **1**, 540–545; (*f*) S. Roquet, A. Cravino, P. Leriche, O. Alévêque, P. Frère and J. Roncali, *J. Am. Chem. Soc.*, 2006, **128**, 3459–3466; (*g*) A. Ajayaghosh, *Chem. Soc. Rev.*, 2003, **32**, 181–191; (*h*) Y. Zhu, R. D. Champion and S. A. Jenekhe, *Macromolecules*, 2006, **39**, 8712–8719; (*i*) E. Zhou, J. Cong, S. Yamakawa, Q. Wei, M. Nakamura, K. Tajima, C. Yang and K. Hashimoto, *Macromolecules*, 2010, **43**, 2873–2879; (*j*) J. Li and Q. Zhang, *ACS Appl. Mater. Interfaces*, 2015, DOI: 10.1021/acsami.5b00113.

20 (*a*) K. R. Justin Thomas, J. T. Lin, Y.-T. Tao and C. H. Chuen, *J. Mater. Chem.*, 2002, **12**, 3516–3522; (*b*) P. Singh, A. Baheti and K. R. J. Thomas, *J. Org. Chem.*, 2011, **76**, 6134–6145.

21 E. Cariati, C. Dragonetti, E. Lucenti, F. Nisic, S. Righetto, D. Roberto and E. Tordin, *Chem. Commun.*, 2014, **50**, 1608–1610.

22 X.-F. Jiang, L. Polavarapu, S. T. Neo, T. Venkatesan and Q.-H. Xu, *J. Phys. Chem. Lett.*, 2012, **3**, 785–790.

23 Y. H. Lee, Y. Yan, L. Polavarapu and Q.-H. Xu, *Appl. Phys. Lett.*, 2009, **95**, 023105.

24 N. Srinivas, S. V. Rao and D. N. Rao, *J. Opt. Soc. Am. B*, 2003, **20**, 2470–2479.

25 (*a*) B. J. Coe, *Chem. – Eur. J.*, 1999, **5**, 2464–2471; (*b*) J. A. Delaire and K. Nakatani, *Chem. Rev.*, 2000, **100**, 1817–1846; (*c*) E. Cariati, C. Dragonetti, E. Lucenti, F. Nisic, S. Righetto, D. Roberto and E. Tordin, *Chem. Commun.*, 2014, **50**, 1608–1610; (*d*) M. P. Cifuentes, M. G. Humphrey, J. P. Morrall, M. Samoc, F. Paul, C. Lapinte and T. Roisnel, *Organometallics*, 2005, **24**, 4280–4288; (*e*) M. P. Cifuentes, C. E. Powell, M. G. Humphrey, G. A. Heath, M. Samoc and B. Luther-Davies, *J. Phys. Chem. A*, 2001, **105**, 9625–9627; (*f*) G. T. Dalton, M. P. Cifuentes, S. Petrie, R. Stranger, M. G. Humphrey and M. Samoc, *J. Am. Chem. Soc.*, 2007, **129**, 11882–11883; (*g*) C. E. Powell, M. P. Cifuentes, J. P. Morrall, R. Stranger, M. G. Humphrey, M. Samoc, B. Luther-Davies and G. A. Heath, *J. Am. Chem. Soc.*, 2003, **125**, 602–610; (*h*) M. Samoc, N. Gauthier, M. P. Cifuentes, F. Paul, C. Lapinte and M. G. Humphrey, *Angew. Chem., Int. Ed.*, 2006, **45**, 7376–7379.

26 (*a*) C. Wang, B. Hu, J. Wang, J. Gao, G. Li, W.-W. Xiong, B. Zou, M. Suzuki, N. Aratani, H. Yamada, F. Huo, P. S. Lee and Q. Zhang, *Chem. – Asian J.*, 2015, **10**, 116–119; (*b*) C. Wang, M. Yamashita, B. Hu, Y. Zhou, J. Wang, J. Wu, F. Huo, P. S. Lee, N. Aratani, H. Yamada and Q. Zhang, *Asian J. Org. Chem.*, 2015, **4**, 646–651; (*c*) C. Wang, J. Wang, P. Li, J. Gao, S. Y. Tan, W. Xiong, B. Hu, P. S. Lee, Y. Zhao and Q. Zhang, *Chem. – Asian J.*, 2014, **9**, 779–783.

27 B. D. Lindner, J. U. Engelhart, O. Tverskoy, A. L. Appleton, F. Rominger, A. Peters, H.-J. Himmel and U. H. F. Bunz, *Angew. Chem., Int. Ed.*, 2011, **50**, 8588–8591.

28 F. Allen, O. Kennard, D. Watson, L. Brammer, A. Orpen and R. Taylor, *J. Chem. Soc., Perkin Trans. 2*, 1987, S1–S19.

29 (*a*) X.-F. Jiang, L. Polavarapu, S. T. Neo, T. Venkatesan and Q.-H. Xu, *J. Phys. Chem. Lett.*, 2012, **3**, 785–790; (*b*) Y. H. Lee, Y. Yan, L. Polavarapu and Q.-H. Xu, *Appl. Phys. Lett.*, 2009, **95**, 023105; (*c*) M. Sheik-Bahae, A. A. Said, T. H. Wei, D. J. Hagan and E. W. Van Stryland, *IEEE J. Quantum Electron.*, 1990, **26**, 760–769.

